

LRO NAC-DERIVED ALBEDO MAP OF SILICIC VOLCANICS. R. N. Clegg-Watkins^{1,2}, B. L. Jolliff¹, and M. J. Watkins³, ¹Department of Earth & Planetary Sciences and the McDonnell Center for the Space Sciences, Washington University in St. Louis, 1 Brookings Dr., St. Louis, MO 63130, ²Planetary Science Institute, Tucson, AZ, ³Engineering Software Research and Development, Inc., St. Louis, MO. (rclegg@levee.wustl.edu)

Introduction: Photometry is an established tool for studying the physical properties of planetary surfaces. Attempts have been made to correlate Hapke photometric parameters and surface physical properties such as roughness and grain size using experiments and simulations [1-6], but the relationship is still not well understood and warrants further study. We have shown that photometric data from Lunar Reconnaissance Orbiter (LRO) Narrow Angle Camera (NAC) images can be used in conjunction with Hapke photometric modeling and laboratory reflectance measurements to make enhanced physical and compositional inferences of surface characteristics [7-9].

Hapke photometric parameter maps have been created using LRO Wide Angle Camera (WAC) data to demonstrate regional photometric variations across the lunar surface and to determine how these variations relate to changes in physical and compositional properties [10]. Here we discuss creating Hapke parameter maps using NAC image data to determine parameter variations at a much finer spatial resolution (~0.5–2 m/pixel) for non-mare (silicic) volcanic regions on the Moon.

Silicic Volcanic Regions. Silicic volcanic areas on the Moon have high reflectance (I/F) and single scattering albedos (w) that are consistent with different proportions of highly reflective minerals including alkali feldspar and quartz, and corresponding low concentrations of mafic minerals [9]. These silicic areas exhibit a range of reflectance values, both within and among the regions, which may have compositional significance. This variation is especially evident at the Compton Belkovich Volcanic Complex (CBVC; 61.1°N, 99.5°E) where features such as volcanic cones and domes are less reflective than some of the other regions in the central portion of the complex [9]. The use of NAC parameter maps allows us to assess how photometric parameters such as w vary on the m-scale and how these variations relate to differences in composition and surface properties at the CBVC.

Methods: To assess how photometric parameters change over a scene, we used Hapke formulations and nonlinear optimization techniques in MATLAB to produce Hapke parameter maps of the CBVC from NAC images. We used a modified form of the Hapke function, optimized from landing site studies [11, 12] as the objective function to be minimized ($h(w)$) for each pixel:

$$h(w) = \left(\frac{w}{4} [p(g) + H(\mu_0, w)H(\mu, w) - 1] [1 + B_{c0}B_c(g, h_c)] S(i, e, \theta) - I_0F/LS \right)^2$$

See [11, 13] for definitions and derivations of the parameters in this equation. This equation was written so that the optimal input parameters should produce a minimum value of $h(w)$ close to, but never less than, 0 for each pixel. The i , e , g , and I/F values were calculated for each pixel by producing backplanes using a NAC Digital Terrain Model (DTM) of the CBVC, which also allowed us to correct for local topography. The MATLAB function *fmincon*, which minimizes a multivariable objective function subject to provided constraints, was used with the interior-point algorithm to solve for w , the parameter of interest. The single scattering albedo has values $0 \leq w \leq 1$, and we used a starting value of $w=0.5$.

We first treated both w and θ (the surface roughness) as variable parameters, but optimal w and θ values could not be found simultaneously because there was no single global minimum in the objective function. This confirms the results of [11], which showed there is no single best pair of (w , θ) values if both are treated as variable parameters. Therefore, we simplified the model by fixing θ at 30° for all image pixels and found the optimal w using a single-variable optimization for each pixel independently. This θ value is similar to that modeled for Apollo 16 background data [11, 12] and is the same value modeled for the background at CBVC using Hapke formulations. Although roughness varies across the complex, we minimize the effects of topography by creating backplanes with the NAC DTM, and we determined 30° was a good starting value to obtain estimates for w .

To minimize the number of free parameters and to determine better fits for w , we held b and c constant at 0.3 and 0.2, respectively (see [12] for more information on how we treat b and c in our models). We set $B_{c0}=0.80$ and $h_c=0.107$, which correspond to values appropriate for the NAC wavelength [14]. The best-fit value of w was then determined for each pixel, with pixels in shadow assigned null values.

Results: The w -map created for a portion of the CBVC is shown in Fig. 1, with a resolution of 2 m/pixel. Shades of blue and blue-green indicate lower values of w , and shades of red indicate higher values (>0.7). Sun-facing slopes and shadowed areas have the

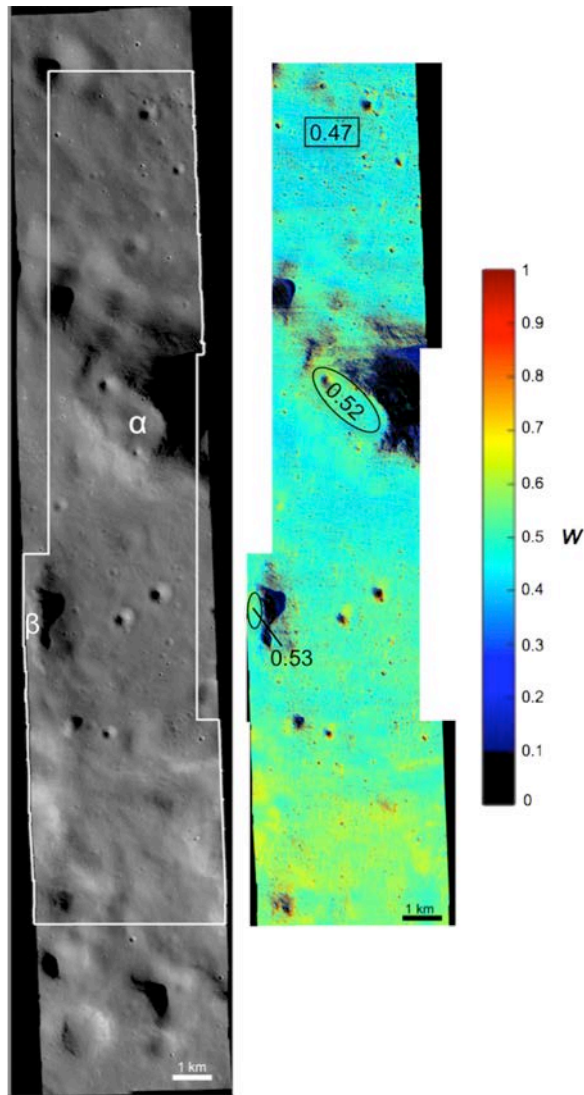


Fig. 1: Hapke w -map for the CBVC. White outline in the NAC image (M103852760R; left) corresponds to the region used to create the w -map. Higher values of w are found in the central part of the complex, indicated by shades of yellow. Annotation on the w -map show values for the α - and β -domes and the background area. Pixels with $w=0-0.1$ correspond to shadows and are assigned null values..

most extreme values. Pixels that fell in shadows of craters or surface features were assigned values of 0 and appear black, and sun-facing slopes appear shades of yellow-orange to red. Aside from areas where we have not completely removed topography, the central part of the complex has the highest w values ($\sim 0.5-0.65$), and these numbers are similar to our modeled values discussed in [7,8]. The region to the north and outside of the complex has lower w values than the complex, with an average value around ~ 0.47 . For comparison, the w modeled for the feldspathic Apollo 16 landing site is 0.48 [11]. Two positive-relief fea-

tures in this region, the α - and β -domes, are 17% and 28% more reflective, respectively, than the background area [9]. As expected, this w -map shows that the α - and β -domes also have smaller w values, 0.51 and 0.53, respectively, than the central part of the complex.

Discussion: Returned sample data and photometric modeling show that soils with the highest plagioclase and lowest mafic mineral contents have the highest reflectance and single scattering albedos. The Compton Belkovich Volcanic Complex has high w values that are consistent with interpretations of felsic minerals and/or glass [8, 9]. Reflectance and w variations are seen within the CBVC, as indicated with the NAC image and w -map shown in Fig. 1, indicating compositional differences exist within the complex [9].

The most reflective regions in the CBVC are low-relief features in the central part of the complex, and these areas have the highest values in the w -map (some highly reflective areas coincide with notable slopes, but not in all cases). The higher I/F and w of these features can be accounted for by more silicic compositions or, as we have shown with laboratory spectra, the addition of up to ~ 20 wt% glassy silicic/rhyolitic materials (pyroclastics) [9]. Lower reflectance values correspond to large constructs such as the α - and β -domes, which likely formed by relatively viscous lavas, perhaps of intermediate compositions such as andesite or dacite. Alternatively, lower silicic glass contents (< 5 wt% according to our laboratory spectral measurements of glassy silicic materials) may explain the lower reflectance of positive-relief features within the complex [9]. Hapke w -maps at the NAC scale reveal that these domes also have lower w values than the central portion of the complex, suggesting that their compositions may be less silicic than the center but more silicic than the background highlands. Variations in reflectance among and within this silicic volcanic complex may be attributed to mixing of felsic components, the presence of KREEPy intermediate lava, and/or associated rhyolitic pyroclastic deposits [9].

References: [1] Mustard J. F. and Pieters C. M. (1989) *JGR*, 94, 13619–13634. [2] McGuire A. F. and Hapke B. W. (1995) *Icarus*, 113, 134–155. [3] Cord A. M. et al. (2003) *Icarus*, 165, 414–427. [4] Denevi B. W. et al. (2008) *JGR*, 113. [5] Shepard M. K. and Helfenstein P. (2011) *Icarus*, 215, 526–533. [6] Souchon A. L. et al. (2011) *Icarus*, 215, 313–331. [7] Clegg R. N. et al. (2014) *LPSC XLV*, Abstract #1256. [8] Clegg R. N. et al. (2014) *LEAG Mtg*, Abstract #3032. [9] Clegg R. N. et al. (2015) *LPSC XLVI*, Abstract #1467. [10] Sato H. et al. (2014) *JGR*, 119, 1775–1805. [11] Clegg R. N. et al. (2014) *Icarus*, 227, 176–194. [12] Clegg-Watkins R. N. et al., *in press*, *Icarus*, doi:10.1016/j.icarus.2015.12.010. [13] Hapke B. (2012) *Cambridge Univ. Press*, 2nd Ed. [14] Hapke B. W. et al. (2012) *JGR*, 117.